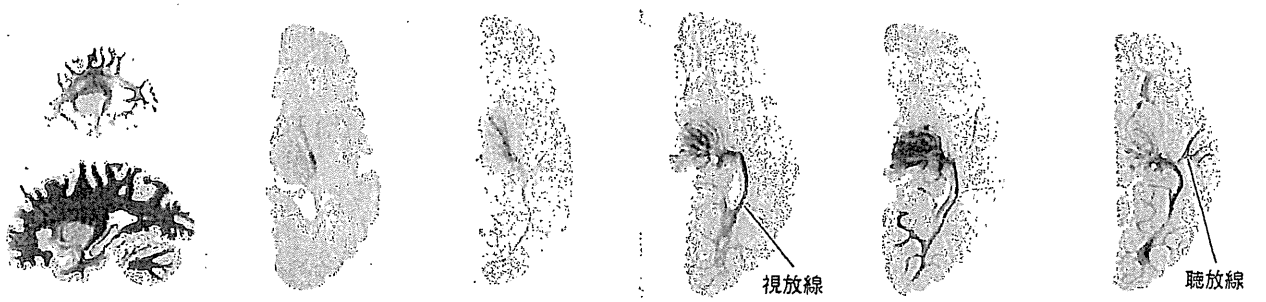

4か月（上段），40歳（下段）　43 cm 胎児　新生児（54 cm）　4週の新生児　7週の新生児　4か月の乳児

図8　Flechsig のヒトの脳の発達における髄鞘化の研究

①視覚神経系は聴覚神経系より早く髄鞘化が完成する

②神経伝達速度は髄鞘化前（軸索）では 3～5 km/時，髄鞘化後で 50～400 km/時

〔8) Sano M, Kuan CC, Kaga K, et al : Early myelination patterns in central auditory pathway of the higher brain : MRI evaluation study. Int J Pediatr Otorhinolaryngol **72** : 1479-1486, 2008〕

おわりに

現在は MRI を用いて，中枢聴覚伝導路および言語中枢の髄鞘化を脳の発達とともにフォローアップすることがわかります。私たちの研究では，中枢聴覚伝導路も言語中枢も難聴の有無にかかわらず，ほぼ古典的な研究と同様に脳の聴覚言語中枢の髄鞘化が完成することがわかりました。これは難聴児の場合，「脳は音刺激の届くことを待っている」ことを示しています。

◎文献◎

1) Darwin C：(渡辺政隆訳) 種の起源．古典新訳文庫　光文社，2009
2) Winston R：(相良倫子訳) 目で見る進化―ダーウィンから DNA まで．さ・え・ら書房，2009
3) 加我君孝，ほか(編)：新臨床耳鼻咽喉科学　第1巻基礎編．中外医学社，2001
4) Weber DB, Fay RR, Popper AN (ed)：The evolutionary biology of hearing. Springer, 1992
5) 加我君孝：感覚器の進化と言語と脳．綜合臨床 **53**：2595-2597, 2004
6) 野村恭也，ほか：耳科学アトラス．シュプリンガージャパン，2008
7) Flechsig P：Anatomie des menschlichen Gehirns und Ruckenmarks auf yelogenetischer Grundlage. Thieme, 1920
8) Sano M, Kuan CC, Kaga K, et al：Early myelination patterns in central auditory pathway of the higher brain：MRI evaluation study. Int J Pediatr Otorhinolaryngol **72**：1479-1486, 2008
9) Su P, Kuan CC, Kaga K, et al：Myelination progression in language-correlated regions in brain of normal children determined by quantitative MRI assessment. Int J Pediatr Otorhinolaryngol **72**：1751-1763, 2008

☆☆☆☆☆　　☆☆☆☆☆

特集 幼少児の難聴の診断・治療と聴こえと言葉のリハビリテーション

聴こえと視力の二重障害児（盲ろう児）

児童発達支援センター（旧難聴幼児通園施設）
富士見台聴こえとことばの教室 内山 勉（うちやま つとむ）

はじめに

まったく見えない「盲児」であっても，聴覚を通じて自分の周囲の様子を知ることができ，また聴覚を通じて音声言語を習得して周囲の人と会話をすることができます。同様にまったく聴覚を使えない「ろう児」であっても，視覚を通じて自分の周囲の様子を知ることができ，動作により周囲の人とかかわりを持つことができます。

もし聴こえと視力の二重障害，すなわち視覚障害と聴覚障害（「難聴」と同義語，以下本文では「聴覚障害」を使用します）が合併したらどうなるでしょうか。聴こえと視力の二重障害の人は自分の身体に触れられる範囲以外はまったく自分の周囲の状況がわからないため，自分のすぐそばにいる人ですらかかわりを持つ（＝コミュニケーションをする）ことができません。このように視覚障害と聴覚障害が合併すると，自分の周囲の状況ですらわからない状態になることから，視覚障害や聴覚障害のみの場合と異なる感覚器の障害といえます[1~3]。このため，欧米では視覚障害と聴覚障害の合併する障害として「盲ろう（Deafblind）」を独立した一つの障害として認定しております[4]。日本でもその流れを受けて，内閣府に設置された「障がい者制度改革推進会議（2009年12月～2011年8月）」では，「盲ろう」を独立した障害として認定しております[4]。

盲ろうの実態

盲ろうに関する全国調査（全国盲ろう者協会調査：平成16～17［2004～2005］年度，図1）では，全国の推定盲ろう児・者総数は16,354人としており，児童は少なく高齢者に多いことが示されています[5]。児童の発生率はきわめて低く，国立特別支援教育総合研究所で行った全国調査（平成11年［1999］視覚・聴覚二重障害を有する児童・生徒の実態調査），および文部科学省が毎年行っている特別支援学級および特別支援学校の在籍児全国調査（視覚障害と聴覚障害と併記された手帳の所持）をもとに推定しますと，聴覚と視覚の二重障害のある児童・生徒の総数は500人程度であり，1学年ごとに40人程度の盲ろう児がいると思われます[4]。

児童の盲ろうになる原因として，Usher症候群（難聴と網膜色素変性症の合併，発症年齢の個人差は大きい），超低出生体重（1,000 g未満），風疹胎内感染，サイトメガロウイルス胎内感染，CHARGE症候群（視力，聴覚，肢体などに障害が多発）などが知られています[2)3)6~8]。

盲ろうの障害の状況については，

著者プロフィール 早稲田大学大学院（心理学専攻）卒業。医学博士（研究分野：難聴乳幼児の聴力検査の信頼性について），言語聴覚士。専門：難聴児・言語発達遅滞児の発達評価。関連著書（分担執筆）に「発達支援学 その理論と実践―育ちが気になる子の子育て支援体系―」（協同医書，2011年）。興味があること：新生児聴覚スクリーニングによって聴覚障害児が乳児期に発見できるようになりましたが，早期発見された聴覚障害児を療育によりどれだけ社会的自立ができるかが今後の興味深い重要な課題だと思っております。

1344-3151/12/¥50/頁/JCOPY

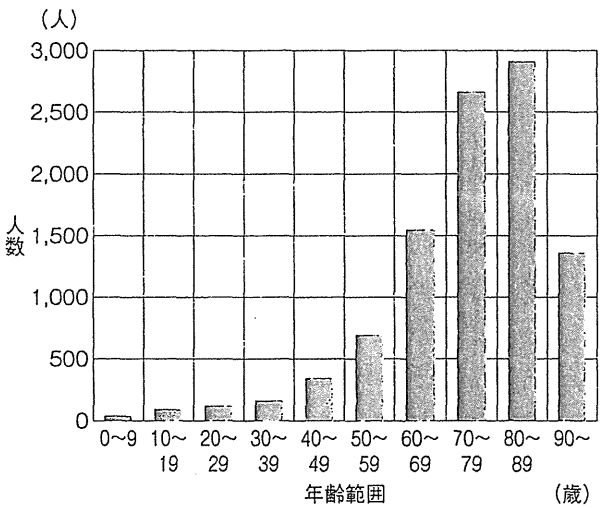

図1 盲ろう者の年齢分布
児童は少なく，高齢者に多いことが示されています。
〔5) 全国盲ろう者協会：平成16/17年度 盲ろう者生活実態調査報告書．平成18年3月〕

視覚障害の程度（完全な盲～弱視）と聴覚障害の程度（最重度～軽度まで）の組合せにより多様です。ただし全盲・全ろう（まったく見えない・聴こえない）の組み合わせは少なく，視覚障害と聴覚障害のうちどちらかがが最重度であり，ほかは中等度の障害である，もしくは両方ともに中等度の障害のであることが多いといわれています。児童の場合は，盲ろうに加えて多くの例で知的障害を合併しており，重症心身障害と判定された児童のなかに盲ろうとして扱うべき児童が少なからず含まれていると推定されています[3)6)]。

周囲からの関与がなければ，盲ろう児は自分の周囲の様子を知ることができません。すぐそばにいる人ともかかわりを持てない状態です。盲ろう児は他者からの支援がなければ食事もできない，訓練を受けなければ生活習慣すべて，さらにコミュニケーション手段や言語（音声言語，手話，指文字，点字，文字）をまったく習得できません。このように盲ろう児は他者からの支援がなければ，自分が感じる範囲での行動をするしかなくなり，動き回る，同じ動きをくり返すなどの自己刺激行動だけとなり，危険をまったく感知できない，他人の介助なしには食べることすらできない状況となります[1)3)6)]。

有名な盲ろう児の例はHelen Keller（ヘレン・ケラー）です。彼女は生後1歳7か月で脳炎により視力と聴力を失った結果，家庭教師Sullvin, A. M.（アン・サリバン）により指文字での指導を受けるまでことばも知らず，野生児のように手探りだけで家の中を動き回っていたといわれています。家庭教師Sullvinは常に彼女に付き添って生活し，触れるもの，嗅ぐものすべてを指文字で入力し続けるなかで，Helen Kellerは触れる物に名前があることを知り，そして自分が感じたことを相手に指文字で伝え，相手からの発信を指文字によって受けられることを理解するようになります。このことから，Helen Kellerは自分の感じる範囲だけの世界から，世の中には自分がいて他者がいること，コミュニケーションによって人同士が通じ合うことを理解し，人間への道を歩み出したのです。このHelen Kellerの例のように，盲ろう児は適切な指導・教育により自立して生活することが可能となるのです[9)]。

盲ろう児の医学的対応と問題点

盲ろう児・者への医学的対応として，視覚障害は眼科で，聴覚障害は耳鼻咽喉科で．その他の診断・治療は内科や小児科で行われるため，統一した診療結果が得られにくい状況です。また「盲ろう児」への医学的な対応が不十分な背景には，乳幼児での視覚障害や聴覚障害の診断のむずかしさがあると思われます。

乳幼児の先天性視覚障害は約4,000人に1人程度であり，精神発達遅滞をともなう例が多数を占めて

著者連絡先 〒117-0034 東京都練馬区富士見台2-34-4 児童発達支援センター（旧難聴幼児通園施設）富士見台聴こえとことばの教室

おります。乳幼児の視覚障害の程度を正確に診断するためには，生理学的検査（視覚誘発反応検査：VEP）以外に，視能訓練士による乳幼児視力検査（乳児がパターンある視標を好んで視ることを利用する視力検査法：PL法）が不可欠ですが，聴覚障害や発達遅滞をともなう場合には視力検査がむずかしくなります。視力障害があると診断されたならば，日常生活場面での行動観察による視機能（視力，色覚，視野，暗順応）の評価をもとに，弱視用眼鏡などによる視力矯正や視能訓練・歩行訓練・日常生活訓練が必要となります。しかし小児眼科の専門医や視能訓練士がいる医療機関や視覚障害児への早期支援ができる施設は全国的に数が限られているのが現状です[7,10]。

先天性の聴覚障害の診療状況も同様です。先天性の聴覚障害は1,000人に1人であり，近年新生児聴覚スクリーニングで乳児期に聴覚障害を発見することが可能になっています。そして，正確な聴力の測定のためには生理学的検査（聴性脳幹反応検査：ABR，耳音響放射検査：OAE）以外に言語聴覚士による乳幼児聴力検査（音が出るとおもちゃが見える条件づけによる聴力検査法：COR法）が不可欠です。発達に問題のない先天性の聴覚障害児は乳児期に発見して補聴器を装用し療育を受けることで，また90dB以上の最重度の難聴がある場合は2歳頃に人工内耳を装用して適切な療育を行うことで，6歳までに年齢相応の言語力を習得して小学校普通学級に就学できます。このように聴覚障害の場合は早期発見・早期療育の効果はあきらかです。なお，聴覚障害に発達遅滞をともなう場合であっても，発達程度に応じた療育効果が期待できます。ただし，療育開始が遅れるとともに言語発達の遅れが目立つようになります。現在のところ，小児耳鼻咽喉科の専門医や聴覚障害児に対応できる言語聴覚士がいる医療機関は全国的にも数が限られ，また児童福祉法に基づきおもに聴覚障害児を療育している通園施設（児童発達支援センター）は全国に20施設程度しかありません。このため，視覚障害を合併した聴覚障害児の早期療育を行える通園施設はさらに少ないと予想されます[8]。

表1 盲ろう児の障害原因と在籍特別支援学校別人数

超低出生体重	14	5	9	12	40
風疹	15	14	5	5	39
中枢性障害	2	2	7	13	24
事故	2	1	4	8	15
不明	48	24	29	54	155
その他	13	7	11	27	58
計	94	53	65	119	331

（人）

盲ろう児がさまざまな特別支援学校に在籍していることがわかります。
〔3）国立特殊教育総合研究所重複障害教育研究部：視覚聴覚二重障害を有する児童・生徒の実態調査報告書．平成12年3月より改変〕

特別支援学校での教育的対応と問題点

盲ろう児への早期支援は公立の視覚障害特別支援学校（盲学校）および聴覚障害特別支援学校（ろう学校）の教育相談および幼稚部で行われています。しかし，盲ろう児の早期支援は医療との連携（視能訓練士等による視力検査・特殊眼鏡装用・視能訓練・歩行訓練，言語聴覚士による聴力検査・補聴器装用・聴能言語訓練）がないまま，教育相談担当教員が指導を行っているのが現状と思われます。

小学校以降の盲ろう児童の就学先については，先の全国調査によると，表1に示すように視覚障害，聴覚障害，知的障害，肢体不自由支援学校などさまざまな学校に在籍しているのが現状です。なお知的水準が高く視覚障害の程度が軽い場合，小学校普通学級に通級している例も

知られています。まれな障害である盲ろうのある児童への教育的な対応については，一部の学校（国立・筑波大付属視覚障害特別支援学校，私立・横浜訓盲学院）を除き，盲ろう児を担当する公立学校の教員の場合，教員の担任替えや転勤があるため，担当教員が盲ろう児にどのように対応するかの教育技術を十分に習得できない状況が継続していると思われます[3]。

盲ろう児への支援の基本

乳児は見る・聴く・触るという経験を積み重ねるなかで，一瞬見たり聴いたりするだけで正確に対象が何かがわかるようになります。たとえば保育園に預けられている乳児は，一瞬見ただけで多くの大人の中から迎えに来た母親を見つけたり，騒がしい保育室の中で母親の声を聴き取ることができるようになります。このように人は一部分を知覚しただけで対象そのものを認知する能力を乳児期から生活のなかで習得していきます（匂いから食べ物がわかる，足音からだれが歩いているかわかる…）。なお，視覚や聴覚については，臨界期（もっとも鋭敏に特定の刺激に反応できる年齢・月齢）のあることが知られており，先天性の白内障では生後 17 週以前に手術をすれば視機能は健全に発達しますが，手術が遅れると視機能が低下したままになることが知られています[7]。また重度の聴覚障害では補聴器や人工内耳装用効果は，3 歳以降になると年齢とともに乏しくなることが確かめられています[8]。このため，感覚器の障害では早期発見・早期療育が強調されています。

強度の弱視があっても，視能訓練を受けることでぼんやり見える物が何かが理解できます。またぼんやりとした輪郭から人とわかれば，視覚障害児は相手に声をかけられます。また聴覚障害児は補聴器もしくは人工内耳を装用して聴能言語訓練を受けることで，相手の発話を聴いたり相手に話しかけたりする，すなわち相手との会話ができるようになります。知的に低い聴覚障害児であっても他者とは動作・サインによりコミュニケーションが可能になります。そこで，盲ろう児の場合，残存する視機能（視力，色覚…）ならびに聴力を最大限活用しつつ，触覚や運動感覚などの感覚を活用して自分の周囲の状況を知る能力を習得することが重要となります。このためには，訓練者は常に盲ろう児の手を取り，話しかける，見せる，触らせるなどのかかわりを行う必要があります。また盲ろう児の障害の程度・状況や発達程度および生活環境に応じて，さまざまな教材や生活のなかでの手がかりを作成し，危険防止への配慮を行う必要があります（図 2）。また家族への具体的な家庭での指導方法や，家族への福祉制度を活用した支援体制（身体障害者手帳の取得，特別児童扶養手当…）の紹介や心理的援助が必要となります[7][8][10]。

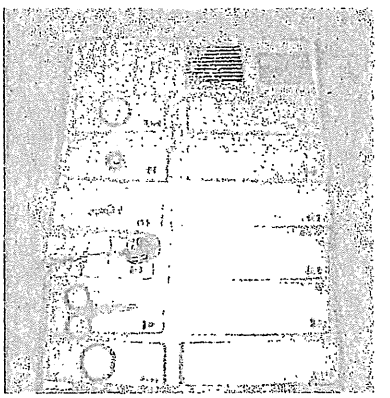

図 2　盲ろう児用教材の 1 例
盲ろう児は手で触れて曜日ごとの時間割を確かめます。青い丸は「朝の会」，鈴は音楽の時間，ネジは作業の時間，スプーンは昼食，はさみは美術の時間，赤い丸は「帰りの会」を示しています。
〔横浜訓盲学院提供〕

筆者は以前盲児・ろう児施設の全国調査を行った際，適切な教育・指導を受けないまま成人となり，知的障害者の成人施設の片隅で一日中常同行動をしている知的障害をともなう盲ろう者を見たことがあります（図 3）。またほぼ同じくらいの障害と思われる盲ろう者ですが，日常生活はどうにか自立し，知的障害者の通所施設に通っている方にも会っています。この二人の盲ろう者での生活能力の差は，幼少時からの家族の養育ならびに教育者・施設指導員に恵まれたか否かの差であることが施設の事例記録からわかり，衝撃を受けました。この 2 事例は，盲ろう児だからこそ適切な早期支援，そして成人までの一貫した教育指導体制が必要なことを示しています[6]。

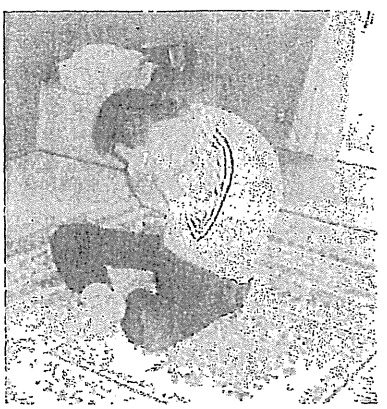

図3 適切な教育・指導を受けないまま成人となり，知的障害者の成人施設の片隅で一日中常同行動をしている知的障害をともなう盲ろう者

相談支援

国立特別支援教育総合研究所では，基本的には教育相談は地域の自治体の教育相談センター等で行う方針ですが，例外として希少障害として「盲ろう児」のみ教育相談（問合せ：http://www.nise.go.jp/cms/6,5,12,92.html）を行っています。また成人の盲ろう者へのサービス機関である全国の都道府県にある盲ろう者友の会でも，盲ろう児への相談や支援を行っています。医療機関としては国立障害者リハビリテーションセンター病院眼科・耳鼻咽喉科および機能回復部門で対応が可能です。また人工内耳等の相談は筆者の属する国立東京医療センター耳鼻咽喉科幼小児難聴クリニックで対応が可能です。

(謝辞)

本稿につきまして，ご教示いただきました前国立特別支援教育総合研究所室長，横浜訓盲学院・学院長 中澤惠江先生に深く感謝いたします。

文献

1) 福島 智：盲ろう者として生きて．明石書店，2011
2) Chen, Deborah：Young Children Who are Deaf-Blind：Implications for Professionals in Deaf and Hard of Hearing Services. The Volta Review **104**, 273-284
3) 国立特殊教育総合研究所重複障害教育研究部：視覚聴覚二重障害を有する児童・生徒の実態調査報告書．平成12年3月
4) 佐藤久夫：障害者総合福祉法の骨格に関する総合福祉部会の提言―新法の制定を目指して―．障がい者制度改革推進会議総合福祉部会報告書．内閣府，平成23年8月
5) 全国盲ろう者協会：平成16 17年度 盲ろう者生活実態調査報告書．平成18年3月
6) 内山 勉：盲児施設・ろうあ児施設に在籍する重複障害児の実態調査ならびに重複障害児の適切な処遇に関する調査研究．こども未来財団委託平成16年児童関連サービス調査研究事業報告書．こども未来財団，平成17年2月
7) 小口芳久：小児眼科のABC．日本医事新報2003
8) 加我君孝：新生児聴覚スクリーニング・早期発見・早期教育のすべて．金原出版，2005
9) 山崎邦夫：年譜で読むヘレン・ケラー ひとりのアメリカ女性の生涯．明石書店，2011
10) 高橋 広：ロービジョンケアの実際．医学書院，2002

☆☆☆☆☆ ☆☆☆☆☆

Acta Oto-Laryngologica, 2012; Early Online, 1–7

informa
healthcare

ORIGINAL ARTICLE

Genetic analysis of *PAX3* for diagnosis of Waardenburg syndrome type I

TATSUO MATSUNAGA[1], HIDEKI MUTAI[1], KAZUNORI NAMBA[1], NORIKO MORITA[2] & SAWAKO MASUDA[3]

[1]*Department of Otolaryngology, Laboratory of Auditory Disorders, National Institute of Sensory Organs, National Tokyo Medical Center, Tokyo,* [2]*Department of Otolaryngology, Teikyo University School of Medicine, Tokyo and* [3]*Department of Otorhinolaryngology, Institute for Clinical Research, National Mie Hospital, Tsu, Japan*

Abstract

Conclusion: PAX3 genetic analysis increased the diagnostic accuracy for Waardenburg syndrome type I (WS1). Analysis of the three-dimensional (3D) structure of PAX3 helped verify the pathogenicity of a missense mutation, and multiple ligation-dependent probe amplification (MLPA) analysis of *PAX3* increased the sensitivity of genetic diagnosis in patients with WS1. *Objectives:* Clinical diagnosis of WS1 is often difficult in individual patients with isolated, mild, or non-specific symptoms. The objective of the present study was to facilitate the accurate diagnosis of WS1 through genetic analysis of *PAX3* and to expand the spectrum of known *PAX3* mutations. *Methods:* In two Japanese families with WS1, we conducted a clinical evaluation of symptoms and genetic analysis, which involved direct sequencing, MLPA analysis, quantitative PCR of *PAX3,* and analysis of the predicted 3D structure of PAX3. The normal-hearing control group comprised 92 subjects who had normal hearing according to pure tone audiometry. *Results:* In one family, direct sequencing of *PAX3* identified a heterozygous mutation, p. I59F. Analysis of PAX3 3D structures indicated that this mutation distorted the DNA-binding site of PAX3. In the other family, MLPA analysis and subsequent quantitative PCR detected a large, heterozygous deletion spanning 1759–2554 kb that eliminated 12–18 genes including a whole *PAX3* gene.

Keywords: *Mutation, MLPA, clinical diagnosis, hearing loss, dystopia canthorum, pigmentary disorder*

Introduction

Waardenburg syndrome (WS) is a hereditary auditory pigmentary disorder that is responsible for 1–3% of congenital deafness cases [1]. WS is classified into four types based on symptoms other than the auditory and pigmentary disorder. Type I WS (WS1) includes dystopia canthorum, and this feature distinguishes WS1 from type II WS. Type III WS is similar to WS1 but is associated with musculoskeletal anomalies of the upper limbs. Type IV WS is similar to type I but is associated with Hirschsprung disease. Diagnostic criteria for WS1 have been proposed [2]. The clinical features of WS1 demonstrate incomplete penetrance and highly varied expression [3,4], which makes diagnosis in individual patients challenging. For example, WS1 patients may present only one isolated symptom. Diagnosis of high nasal root and medial eyebrow flare can be difficult when they are mild. Hearing loss and early graying are relatively common in the general population and are not specific to WS1. Thus, the accuracy of WS1 diagnosis needs to be improved by the use of additional diagnostic procedures.

It is reported that more than 90% of patients with WS1 harbor point mutations in *PAX3* [5], and an additional 6% of WS1 patients harbor partial or complete *PAX3* deletions [6]. This high frequency of *PAX3* mutation in WS1 suggests that clinical diagnosis of WS1 could be facilitated by *PAX3* genetic analysis. To date, more than 80 *PAX3*

Correspondence: Tatsuo Matsunaga, Department of Otolaryngology, Laboratory of Auditory Disorders, National Institute of Sensory Organs, National Tokyo Medical Center, 2-5-1 Higashigaoka, Meguro, Tokyo, 152-8902, Japan. Tel: +81 3 3411 0111. Fax: +81 3 3412 9811. E-mail: matsunagatatsuo@kankakuki.go.jp

This study was presented at the annual meeting of the Collegium Oto-Rhino-Laryngologicum Amicitiae Sacrum, Rome, August 28, 2012.

(Received 19 September 2012; accepted 20 October 2012)

ISSN 0001-6489 print/ISSN 1651-2251 online © 2012 Informa Healthcare
DOI: 10.3109/00016489.2012.744470

mutations are reported to be associated with WS1 [5]. A de novo paracentric inversion on chromosome 2 in a Japanese child with WS1 provided a clue for identification of *PAX3* in the distal part of chromosome 2 [7]. However, only a few *PAX3* mutations including the chromosomal inversion have been reported in Japanese patients with WS1 since then [8,9].

In the present study, we conducted *PAX3* genetic analysis to facilitate diagnosis of WS1 in two Japanese families. In one family, to verify the pathogenicity of an identified missense mutation, we analyzed the effect of the mutation on the three-dimensional (3D) structure of PAX3. In the other family, no mutations were identified by direct sequencing, so multiple ligation-dependent probe amplification (MLPA) analysis was used to search for large deletions in *PAX3* and thereby increase the sensitivity of genetic diagnosis.

Material and methods

Patients and control subjects

Two Japanese families with WS1 were included in the study. The diagnosis of WS1 was based on criteria proposed by the Waardenburg Consortium [2]. The normal-hearing controls comprised 92 subjects who had normal hearing according to pure tone audiometry. This study was approved by the institutional ethics review board at the National Tokyo Medical Center. Written informed consent was obtained from all subjects included in the study or from their parents.

Clinical evaluation

A comprehensive clinical history was taken from subjects who were examined at our hospitals or from their parents. During physical examination, special attention was given to the color of the skin, hair, and iris, and to other anomalies such as dystopia canthorum, medial eyebrow flare, limb abnormalities, and Hirschsprung disease. After otoscopic examination, behavioral audiometric testing was performed. The test protocol was selected according to the developmental age of the subject (conditioned orientation response audiometry, play audiometry, or conventional audiometric testing, from 125 to 8000 Hz), and testing was performed using a diagnostic audiometer in a soundproof room. Auditory brainstem response (ABR) and otoacoustic emission were also evaluated in some subjects.

Direct sequencing

Genomic DNA from the subjects was extracted from peripheral blood leukocytes using the Gentra Puregene® Blood kit (QIAGEN, Hamburg, Germany). Mutation screening of *PAX3* was performed by bidirectional sequencing of each exon (exons 1–11) together with the flanking intronic regions using an ABI 3730 Genetic Analyzer (Applied Biosystems, Foster City, CA, USA). Primer sequences for *PAX3* are listed in Table I. Mutation nomenclature is based on the genomic DNA sequence of [GenBank accession no. NG_011632.1], with the A of the translation initiation codon considered as +1. Nucleotide conservation between mammalian species was evaluated using ClustalW (http://www.ebi.ac.uk/Tools/msa/clustalw2/). PolyPhen-2 software (http://genetics.bwh.harvard.edu/pph2/) was used to predict the functional consequence(s) of each amino acid substitution.

MLPA

MLPA analysis was performed using an MLPA kit targeting *PAX3*, *MITF*, and *SOX10* (SALSA MLPA Kit P186-B1, MRC-Holland, Amsterdam, The Netherlands) according to the manufacturer's protocol. Exon-specific MLPA probes for exons 1–9 of *PAX3* and control probes were hybridized to genomic DNA from the subjects and normal controls and ligated with fluorescently labeled primers. A PCR reaction was then performed to amplify the hybridized probes. The amplified probes were fractionated on an ABI3130xl Genetic Analyzer (Applied Biosystems) and the peak patterns were evaluated using GeneMapper (Applied Biosystems).

Real-time PCR

To determine the length of each deleted genomic region, 100 ng of genomic DNA from the subjects and a normal control were subjected to quantitative PCR (Prism 7000, Applied Biosystems) using Power SYBR® Green Master Mix (Life Technologies, Carlsbad, CA, USA) and 12 sets of primers designed to amplify sequence-tagged sites on chromosome 2 (GenBank accession nos: RH46518, RH30035, RH66441, GDB603632, 1988, RH24952, RH47422, RH65573, RH26526, RH35885, RH16314, and RH92249).

Homology modeling of the PAX3 paired domain

The DNA-binding site of the paired domain of PAX3 was modeled using SWISS-MODEL [10] with the crystal structure of the PAX5 paired domain-DNA complex (PDB ID:1PDN_chain C) as the template because PAX3 and PAX5 are functionally and structurally similar [11]. The amino acid

Table I. Primer sequences for *PAX3*.

Exon 1	Forward	5′-TGTAAAACGACGGCCAGTAGAGCAGCGCGCTCCATTTG-3′
	Reverse	5′-CAGGAAACAGCTATGACCGCTCGCCGTGGCTCTCTGA-3′
Exon 2	Forward	5′-TGTAAAACGACGGCCAGTAAGAAGTGTCCAGGGCGCGT-3′
	Reverse	5′-CAGGAAACAGCTATGACCGGTCTGGGTCTGGGAGTCCG-3′
Exon 3	Forward	5′-TGTAAAACGACGGCCAGTTAAACGCTCTGCCTCCGCCT-3′
	Reverse	5′-CAGGAAACAGCTATGACCGGGATGTGTTCTGGTCTGCCC-3′
Exon 4	Forward	5′-TGTAAAACGACGGCCAGTAATGGCAACAGAGTGAGAGCTTCC-3′
	Reverse	5′-CAGGAAACAGCTATGACCAGGAGACACCCGCGAGCAGT-3′
Exon 5	Forward	5′-TGTAAAACGACGGCCAGTGGTGCCAGCACTCTAAGAACCCA-3′
	Reverse	5′-CAGGAAACAGCTATGACCGGTGATCTGACGGCAGCCAA-3′
Exon 6	Forward	5′-TGTAAAACGACGGCCAGTTGCATCCCTAGTAAAGGGCCA-3′
	Reverse	5′-CAGGAAACAGCTATGACCGGTGTCCATGGAAGACATTGGG-3′
Exon 7	Forward	5′-AACTATTATTTCATCAGTGAAATC-3′
	Reverse	5′-ATTCACTTGTATAAAATATCCACC-3′
Exon 8	Forward	5′-TGTAAAACGACGGCCAGTTGAAGCCAGTAGGAAGGGTGGA-3′
	Reverse	5′-CAGGAAACAGCTATGACCTGCAGGTTAAGAAACGCAGTTTGA-3′
Exon 9a	Forward	5′-TGTAAAACGACGGCCAGTTTGATACCGGCATGTGTGGC-3′
	Reverse	5′-CAGGAAACAGCTATGACCTGCAGTCAGATGTTATCGTCGGG-3′
Exon 9b	Forward	5′-TGTAAAACGACGGCCAGTCACAACTTTGTGTCCCTGGGATT-3′
	Reverse	5′-CAGGAAACAGCTATGACCGGGACTCCTGACCAACCACG-3′
Exon 10–11	Forward	5′-TGTAAAACGACGGCCAGTGCAAATGGAATGTTCTAGCTCCTCG-3′
	Reverse	5′-CAGGAAACAGCTATGACCGGTCAGCTCCAGGATCATATGGG-3′

sequences of the PAX3 and PAX5 paired domains were 79% homologous. The predicted PAX3 structure and the p.I59F mutation structure were superimposed on the backbone atoms of the PAX5 paired domain-DNA complex and displayed using the extensible visualization system, UCSF Chimera [12].

Results

In family 1, the proband, a 9-month-old male, was the first child of unrelated Japanese parents. Abnormal responses were found upon newborn hearing screening in the left ear, and left hearing loss was diagnosed by ABR. On physical examination, dystopia canthorum was noted, with a W-index of 2.77. The patient's mother also had dystopia canthorum, with a W-index of 2.68. She also had a history of early graying that started at age 16 years. She had not been diagnosed with WS1. According to the parents, 10 members of this family, including the proband and the mother, showed clinical features consistent with WS1 (Figure 1). ABR performed in the proband

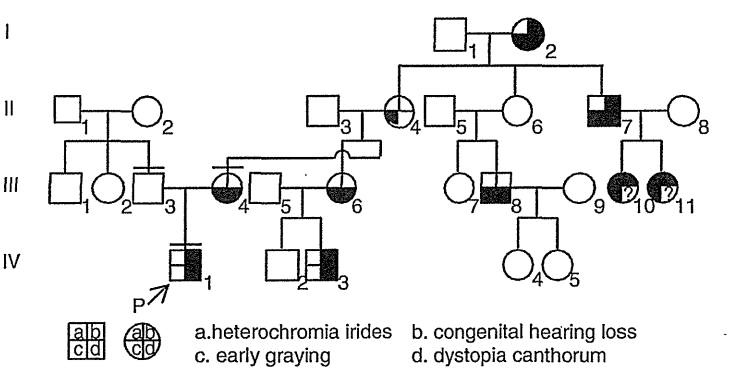

Figure 1. Pedigree of family 1. The proband is indicated by an arrow. The individuals we examined personally are indicated by a bar over the symbol. Phenotypes observed in this family are indicated symbolically as detailed below the pedigree.

revealed normal hearing in the right ear and no responses to 105 dB click stimuli in the left ear. Computed tomography (CT) of the temporal bone showed normal structures in the inner, middle, and outer ears.

Genetic analysis of *PAX3* was conducted in this family, and direct sequencing of *PAX3* revealed a heterozygous mutation, c.175A>T, in the proband and his mother. This mutation resulted in a missense mutation, p.I59F (Figure 2A). The proband's father did not harbor this mutation. p.I59F is located within exon 2 and is part of the paired domain of *PAX3*, which is a critical region for interaction between transcription factors and target DNA (Figure 2B). A multiple alignment of *PAX3* orthologs at this region demonstrated that I59 was evolutionarily conserved among various species (Figure 2C). The p.I59F mutation was not identified in any of the 184 alleles from the normal control subjects. This mutation was predicted to be 'probably damaging' according to PolyPhen-2 software.

The predicted 3D structures of the paired domain of the PAX3-DNA complex indicated that the PAX3 paired domain binds to the corresponding DNA (white double helixes) via hydrogen bonds (pink lines) at the N-terminal of α-helix1 (H1), α-helix2 (H2), and α-helix3 (H3) (indicated in blue; Figure 3A). I59 is located in the middle of H1, H2, and H3 and is surrounded by hydrophobic residues (green) protruding from H1, H2, and H3. Because the van der Waals radius of phenylalanine (Figure 3C; white arrows) is larger than that of isoleucine (Figure 3B, white arrowheads), F59 repels the surrounding hydrophobic residues by van der Waals forces and increases the distance between F59 and the surrounding hydrophobic residues, resulting in structural distortion of the DNA-binding site of PAX3. Since this site is precisely shaped for maximal binding to the corresponding DNA, this mutation is likely to reduce the binding ability of the paired domain of PAX3 and cause WSI. A mutational search found the same mutation in another Japanese family [8].

In family 2, the proband, a female aged 4 years and 4 months, was the first child of unrelated Japanese parents. Abnormal responses were found upon newborn hearing screening in the right ear, and right hearing loss was diagnosed by ABR. On physical examination, dystopia canthorum, medial eyebrow flare, and a white forelock were noted. She was admitted to hospital suffering from ketotic hypoglycemia of unknown cause when aged 4 years. Her mother presented with heterochromia iridis, dystopia canthorum, and medial eyebrow flare, and her grandmother presented with early graying that started at around 20 years of age, dystopia canthorum, and

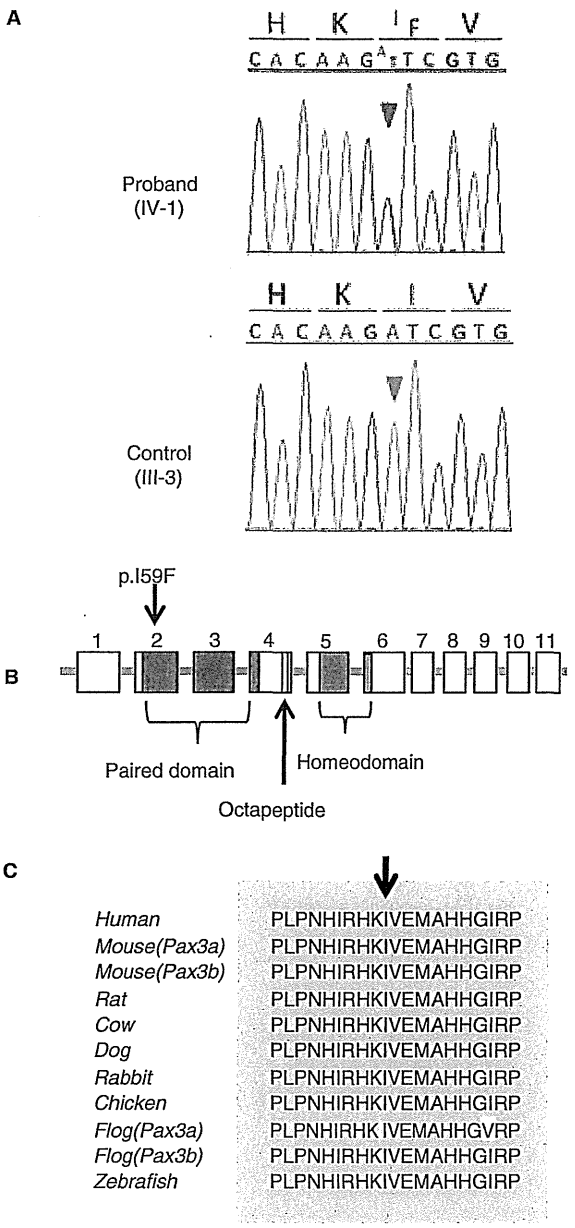

Figure 2. The p.I59F mutation of *PAX3* detected in family 1. (A) Sequence chromatogram for the proband and unaffected control. A heterozygous A to T transversion (red arrowhead) that changes codon 59 from ATC, encoding isoleucine (I), to TTC, encoding phenylalanine (F), was detected in the proband but not in the control (green arrowhead). (B) Localization of the p.I59F mutation and functional domains of PAX3. (C) A multiple alignment of PAX3 orthologs. Regions of amino acid sequence identity are shaded gray. The position of I59 is indicated by an arrow and shaded yellow.

medial eyebrow flare. According to the grandmother, the father of the grandmother also had dystopia canthorum and medial eyebrow flare. The pedigree of family 2 is shown in Figure 4. The grandmother

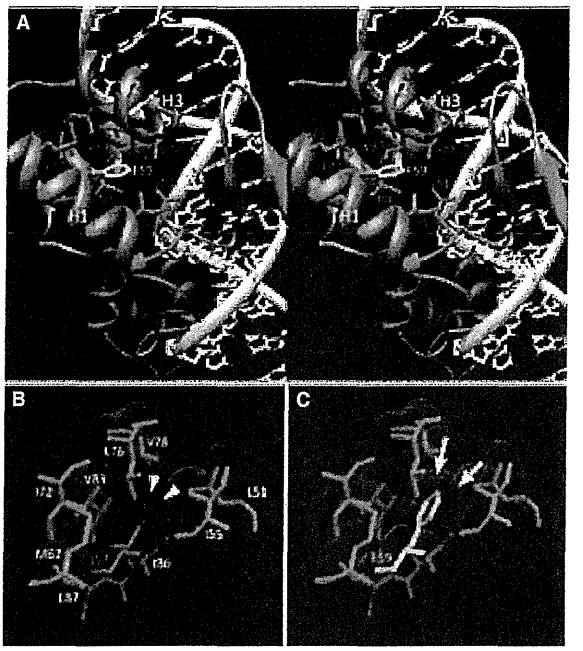

Figure 3. The predicted structure of the PAX3 paired domain-DNA complex. (A) The stereo view indicates that the mutated residue was surrounded by hydrophobic residues (green) protruding from H1, H2, and H3 of the paired domain (blue), which binds to DNA (white, sugar; blue, nitrogen; red, oxygen). The pink lines indicate hydrogen bonds. Magenta and yellow residues indicate I59 and F59, respectively. (B, C) The colored spheres indicate the van der Waals surface boundaries, the radius of the hydrophobic residues is shown in green, I59 is shown in magenta and is also indicated by arrowheads, and F59 is shown in yellow and is also indicated by arrows.

and her father had never been diagnosed with WS1. Pure tone audiometry of the proband showed severe hearing loss in the right ear and normal hearing in the left ear. The results of ABR and distortion product otoacoustic emissions in the proband were compatible with those obtained for pure tone audiometry.

Because direct sequencing of *PAX3* in the proband and her grandmother revealed no mutations, we conducted MLPA analysis to search for a large deletion of *PAX3*, and found that the copy number of all tested exons (exons 1–9) of *PAX3* was half that of the number of other chromosomal regions in both subjects (Figure 5A). In control subjects, all tested exons of *PAX3* showed the same copy number as the other chromosomal regions (Figure 5B). To determine the size of the deleted region, quantitative PCR was performed at 12 sequence-tagged sites on chromosome 2q36, which includes *PAX3*. In the proband, copy numbers at nine sites in the middle of the tested region (white arrows) were half that of those examined in normal controls, but the copy numbers at three of the sites near the 5' and 3' ends of the tested region (black arrows) were identical to those examined in normal controls (Figure 6). This result demonstrated that the chromosomal region spanning 1759–2554 kb at 2q36, which includes the whole *PAX3* gene, was deleted in one of the alleles of the proband. The same results were detected in the grandmother. A search for the deleted region revealed that this region contained between 12 and 18 genes, including *PAX3*.

Discussion

The heterozygous missense mutation, p.I59F, was identified in family 1. The pathogenicity of a novel or rare missense mutation in the causative gene is not necessarily verified even when the mutation is absent from a large number of normal controls, when the residue is evolutionary conserved among different species, or if the mutation is associated with the phenotype within a family, because an identified

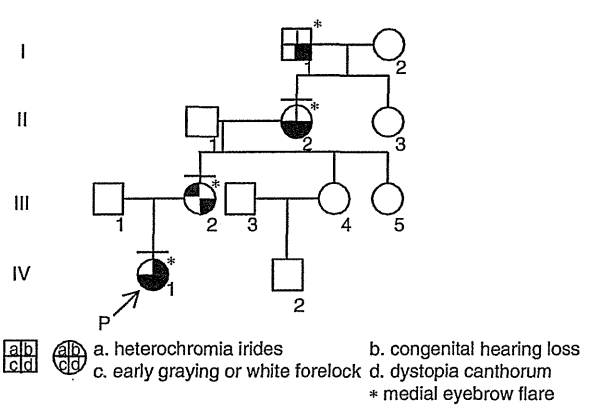

Figure 4. Pedigree of family 2. The proband is indicated by an arrow. The individuals we examined personally are indicated by a bar over the symbol. Phenotypes observed in this family are indicated symbolically, as detailed below the pedigree.

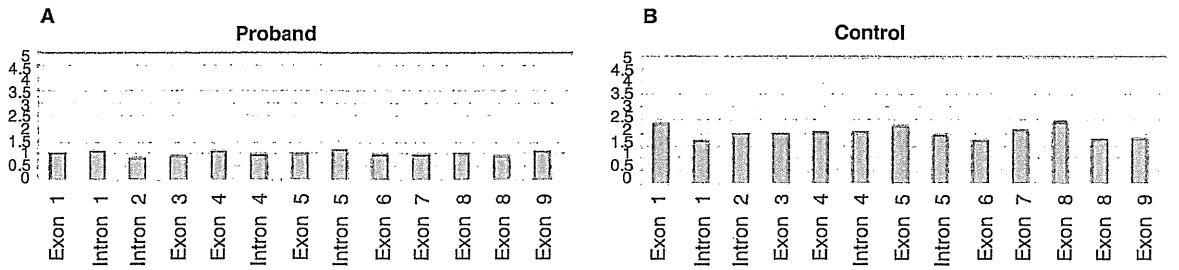

Figure 5. Results of MLPA analysis of *PAX3* in family 2. (A, B) Relative ratios of DNA quantity in each exon compared with that in the control region are shown for the proband (A) and control (B).

missense mutation may be a rare normal variant. Thus, the pathogenicity of such mutations needs to be verified by detection of the same mutation in multiple families with the same phenotype or by functional analysis. The functional consequences of a few *PAX3* mutations have been tested and reduced DNA-binding properties have been reported [13–15]. The p.I59F mutation was reported in a Japanese family [8], but functional analysis has not been conducted. We analyzed the predicted 3D structures of the paired domain of the PAX3-DNA complex and showed that this mutation was likely to distort the structure of the DNA-binding site of PAX3 and lead to functional impairment. This result substantially supports the hypothesis that the p.I59F mutation is pathogenic, although it is based on a theoretical prediction rather than functional experiments.

In family 2, the distinct phenotypes of the proband, the proband's mother, and the proband's grandmother were congenital unilateral hearing loss, heterochromia iridis, and early graying, respectively. Because of these differences, they were not aware of the hereditary nature of the symptoms. Identification of the *PAX3* mutation in the proband and the proband's grandmother led to an accurate diagnosis of WS1 and facilitated understanding of the symptoms. In this family, direct sequencing of *PAX3* did not detect any mutations, but MLPA analysis detected a large heterozygous deletion. Furthermore, quantitative PCR analysis revealed that the deleted region spanned 1759–2554 kb and included 12–18 genes. Large deletions of *PAX3* in patients with WS1 have been reported in several families [6,16–18]. To our knowledge, however, this is the largest deletion identified in patients with WS1 and has, therefore, expanded the spectrum of *PAX3* mutations. There is no reported correlation between the nature of the mutation (deleted vs truncated or missense) or

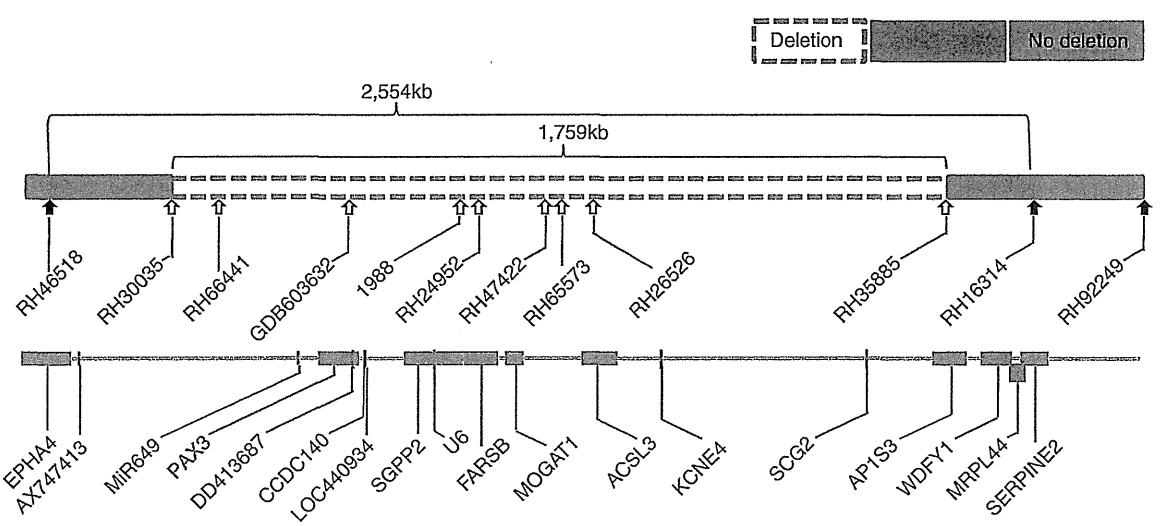

Figure 6. Genetic map showing the estimated location of the *PAX3* deletion together with the regions surrounding *PAX3*. Sites examined by quantitative PCR are indicated by arrows. Blank and white arrows indicate that the quantities of DNA at these sites are half or identical to the quantities of DNA at the corresponding sites in the control, respectively. The 5' and 3' ends of the deletion are located within the blue regions flanking the white region, designated as 'deletion,' and flanked by the green regions, designated as 'no deletion.' All genes mapped within this region, including *PAX3*, are shown in the lower map.

its location in *PAX3*, and the severity of the WS1 phenotype [19,20]. Similarly, no evidence of such a correlation was found in the data presented in this study.

In the present study, *PAX3* genetic diagnosis contributed to the accurate diagnosis of WS1. Such diagnosis could help provide genetic counseling to patients with isolated or few phenotypic symptoms, those with mild phenotypes or few first-degree relatives, or those who have yet to develop any symptoms. In addition, analysis of the predicted 3D structure of PAX3 facilitated the verification of pathogenicity of a missense mutation, and MLPA analysis increased the sensitivity of genetic diagnosis of WS1.

Acknowledgments

We thank the families that participated in this study. This study was supported by a Grant-in-Aid for Clinical Research from the National Hospital Organization, and by a Health and Labour Sciences Research Grants for Research on Rare and Intractable Diseases from the Ministry of Health, Labour and Welfare of Japan.

Declaration of interest: The authors report no conflicts of interest. The authors alone are responsible for the content and writing of the paper.

References

[1] Read AP, Newton VE. Waardenburg syndrome. J Med Genet 1997;34:656–65.

[2] Farrer LA, Grundfast KM, Amos J, Arnos KS, Asher JH Jr, Beighton P, et al. Waardenburg syndrome (WS) type I is caused by defects at multiple loci, one of which is near ALPP on chromosome 2: first report of the WS consortium. Am J Hum Genet 1992;50:902–13.

[3] Liu XZ, Newton VE, Read AP. Waardenburg syndrome type II: phenotypic findings and diagnostic criteria. Am J Med Genet 1995;55:95–100.

[4] Pardono E, van Bever Y, van den Ende J, Havrenne PC, Iughetti P, Maestrelli SR, et al. Waardenburg syndrome: clinical differentiation between types I and II. Am J Med Genet A 2003;117A:223–35.

[5] Pingault V, Ente D, Dastot-Le Moal F, Goossens M, Marlin S, Bondurand N. Review and update of mutations causing Waardenburg syndrome. Hum Mutat 2010;31: 391–406.

[6] Milunsky JM, Maher TA, Ito M, Milunsky A. The value of MLPA in Waardenburg syndrome. Genet Test 2007;11:179–82.

[7] Ishikiriyama S, Tonoki H, Shibuya Y, Chin S, Harada N, Abe K, et al. Waardenburg syndrome type I in a child with de novo inversion (2)(q35q37.3). Am J Med Genet 1989;33: 505–7.

[8] Soejima H, Fujimoto M, Tsukamoto K, Matsumoto N, Yoshiura KI, Fukushima Y, et al. Three novel PAX3 mutations observed in patients with Waardenburg syndrome type 1. Hum Mutat 1997;9:177–80.

[9] Kashima T, Akiyama H, Kishi S. Asymmetric severity of diabetic retinopathy in Waardenburg syndrome. Clin Ophthalmol 2011;5:1717–20.

[10] Kiefer F, Arnold K, Kunzli M, Bordoli L, Schwede T. The SWISS-MODEL Repository and associated resources. Nucleic Acids Res 2009;37:D387–92.

[11] Xu W, Rould MA, Jun S, Desplan C, Pabo CO. Crystal structure of a paired domain-DNA complex at 2. 5 A resolution reveals structural basis for Pax developmental mutations. Cell 1995;80:639–50.

[12] Pettersen EF, Goddard TD, Huang CC, Couch GS, Greenblatt DM, Meng EC, et al. UCSF Chimera – a visualization system for exploratory research and analysis. J Comput Chem 2004;25:1605–12.

[13] Chalepakis G, Goulding M, Read A, Strachan T, Gruss P. Molecular basis of splotch and Waardenburg Pax-3-mutations. Proc Natl Acad Sci USA 1994;91:3685–9.

[14] Corry GN, Underhill DA. Pax3 target gene recognition occurs through distinct modes that are differentially affected by disease-associated mutations. Pigment Cell Res 2005;18: 427–38.

[15] Fortin AS, Underhill DA, Gros P. Reciprocal effect of Waardenburg syndrome mutations on DNA binding by the Pax-3 paired domain and homeodomain. Hum Mol Genet 1997;6:1781–90.

[16] Baldwin CT, Lipsky NR, Hoth CF, Cohen T, Mamuya W, Milunsky A. Mutations in PAX3 associated with Waardenburg syndrome type I. Hum Mutat 1994;3:205–11.

[17] Tassabehji M, Newton VE, Leverton K, Turnbull K, Seemanova E, Kunze J, et al. PAX3 gene structure and mutations: close analogies between Waardenburg syndrome and the Splotch mouse. Hum Mol Genet 1994;3: 1069–74.

[18] Wang J, Li S, Xiao X, Wang P, Guo X, Zhang Q. PAX3 mutations and clinical characteristics in Chinese patients with Waardenburg syndrome type 1. Mol Vis 2010;16:1146–53.

[19] Baldwin CT, Hoth CF, Macina RA, Milunsky A. Mutations in PAX3 that cause Waardenburg syndrome type I: ten new mutations and review of the literature. Am J Med Genet 1995;58:115–22.

[20] Tassabehji M, Newton VE, Liu XZ, Brady A, Donnai D, Krajewska-Walasek M, et al. The mutational spectrum in Waardenburg syndrome. Hum Mol Genet 1995;4: 2131–7.

CLINICAL GENETICS An International Journal of Genetics, Molecular and Personalized Medicine

Clin Genet 2012: 82: 425–432
Printed in Singapore. All rights reserved

CLINICAL GENETICS
doi: 10.1111/j.1399-0004.2012.01897.x

Original Article

A prevalent founder mutation and genotype–phenotype correlations of *OTOF* in Japanese patients with auditory neuropathy

T Matsunaga[a], H Mutai[a], S Kunishima[b], K Namba[a], N Morimoto[c], Y Shinjo[d], Y Arimoto[e], Y Kataoka[f], T Shintani[g], N Morita[h], T Sugiuchi[i], S Masuda[j], A Nakano[e], H Taiji[c] and K Kaga[d]

[a]Laboratory of Auditory Disorders, National Institute of Sensory Organs, National Tokyo Medical Center, Tokyo, Japan, [b]Department of Advanced Diagnosis, Clinical Research Center, National Hospital Organization Nagoya Medical Center, Nagoya, Japan, [c]Department of Otorhinolaryngology, National Center for Child Health and Development, Tokyo, Japan, [d]National Institute of Sensory Organs, National Hospital Organization Tokyo Medical Center, Tokyo, Japan, [e]Division of Otorhinolaryngology, Chiba Children's Hospital, Chiba, Japan, [f]Department of Otolaryngology, Head and Neck Surgery, Okayama University Postgraduate School of Medicine, Dentistry and Pharmaceutical Science, Okayama, Japan, [g]Department of Otolaryngology, Sapporo Medical University School of Medicine, Sapporo, Japan, [h]Department of Otolaryngology, Teikyo University School of Medicine, Tokyo, Japan, [i]Department of Otolaryngology, Kanto Rosai Hospital, Kawasaki, Japan, and [j]Department of Otorhinolaryngology, Institute for Clinical Research, National Mie Hospital, Tsu, Japan

Key words: auditory neuropathy – genotype–phenotype correlation – mutation – non-syndromic hearing loss – *OTOF*

Corresponding author: Tatsuo Matsunaga MD, PhD, Laboratory of Auditory Disorders and Department of Otolaryngology, National Institute of Sensory Organs, National Tokyo Medical Center, 2-5-1 Higashigaoka, Meguro, Tokyo 152-8902, Japan.

Matsunaga T, Mutai H, Kunishima S, Namba K, Morimoto N, Shinjo Y, Arimoto Y, Kataoka Y, Shintani T, Morita N, Sugiuchi T, Masuda S, Nakano A, Taiji H, Kaga K. A prevalent founder mutation and genotype–phenotype correlations of *OTOF* in Japanese patients with auditory neuropathy.
Clin Genet 2012: 82: 425–432. © John Wiley & Sons A/S, 2012

Auditory neuropathy is a hearing disorder characterized by normal outer hair cell function and abnormal neural conduction of the auditory pathway. Aetiology and clinical presentation of congenital or early-onset auditory neuropathy are heterogeneous, and their correlations are not well understood. Genetic backgrounds and associated phenotypes of congenital or early-onset auditory neuropathy were investigated by systematically screening a cohort of 23 patients from unrelated Japanese families. Of the 23 patients, 13 (56.5%) had biallelic mutations in *OTOF*, whereas little or no association was detected with *GJB2* or *PJVK*, respectively. Nine different mutations of *OTOF* were detected, and seven of them were novel. p.R1939Q, which was previously reported in one family in the United States, was found in 13 of the 23 patients (56.5%), and a founder effect was determined for this mutation. p.R1939Q homozygotes and compound heterozygotes of p.R1939Q and truncating mutations or a putative splice site mutation presented with stable, and severe-to-profound hearing loss with a flat or gently sloping audiogram, whereas patients who had non-truncating mutations except for p.R1939Q presented with moderate hearing loss with a steeply sloping, gently sloping or flat audiogram, or temperature-sensitive auditory neuropathy. These results support the clinical significance of comprehensive mutation screening for auditory neuropathy.

Conflict of interest

The authors declare no conflict of interest.

Tel.:+81 3 3411 0111;
fax:+81 3 3412 9811;
e-mail:
matsunagatatsuo@kankakuki.go.jp

Received 28 February 2012, revised and accepted for publication 6 April 2012

Auditory neuropathy (AN) is a hearing disorder characterized by normal outer hair cell function, as revealed by the presence of otoacoustic emissions (OAE) or cochlear microphonics, and abnormal neural conduction of the auditory pathway, as revealed by the absence or severe abnormality of auditory brainstem responses (ABR) (1). Hearing disorders having the same characteristics have also been reported as auditory nerve disease in adult cases (2). Individuals with AN invariably have difficulties in understanding speech (3), and approximately 10% of infants diagnosed with profound hearing loss have AN (3, 4).

About 50% of subjects with congenital or early-onset AN have risk factors such as perinatal hypoxia, whereas the remaining 50% of subjects are likely to have a genetic factor (3, 5). To date, four loci responsible for non-syndromic AN have been mapped: DFNB9 caused by *OTOF* mutation and DFNB59 caused by *PJVK* mutation, both of which are responsible for autosomal recessive AN; AUNA1 caused by DIAPH3 mutation, which is responsible for autosomal dominant AN; and AUNX1, which is responsible for X-linked AN (6–9). Mutations in *OTOF*, which contains 50 exons and encodes short and long isoforms of otoferlin (10), are the most frequent mutations associated with AN with various frequency depending on the population studied (11–15). Most *OTOF* genotypes have been associated with stable, severe-to-profound hearing loss with only a few exceptions (11–20). Studies of genetic backgrounds and clinical phenotypes in various populations will extend our knowledge of genotype–phenotype correlations and may help in the management and treatment of AN.

Materials and methods

Subjects

We enrolled 23 index patients of unrelated Japanese families with congenital or early-onset AN. Diagnosis of hearing loss was made by age 2 in all patients except for one, who had mild hearing loss diagnosed at age 9. All patients had non-syndromic AN in both ears, and they were collected from all over Japan as part of a multicentre study of AN. Patients with hearing loss of possible environmental risk factors for AN such as neonatal hypoxia or jaundice were excluded. With regard to the family history, one patient had a brother having congenital AN and all others were simplex. DNA samples and medical information were obtained from each proband and, if possible, parents and siblings. For DNA samples, 2 parents, 1 parent, no parent, and 1 sibling were available in 10 families, 4 families, 9 families, and 1 family, respectively. None of parents of 23 index patients complained of hearing loss by clinical interview. For the normal-hearing control, 189 subjects who had normal hearing by pure-tone audiometry were used. This study was approved by the institutional ethics review board at the National Tokyo Medical Center. Written informed consent was obtained from all the subjects included in the study or their parents.

Genetic analysis

DNA was extracted from peripheral blood by standard procedures. Genetic analysis for mutations in *GJB2* and for A1555G and A3243G mitochondrial DNA mutations were conducted in all patients according to published methods (21, 22). Mutation screening of *OTOF* was performed by bidirectional sequencing of amplicons generated by PCR amplification of each exon (exons 1–50) and splice sites using an ABI 3730 Genetic Analyzer (Applied Biosystems, Foster City, CA). Primer sequences for *OTOF* are listed in Table S1, supporting information. Mutation nomenclature is based on genomic DNA sequence (GenBank accession number NG_009937.1), with the A of the translation initiation codon considered as +1. The nucleotide conservation between mammalian species was evaluated by ClustalW (http://www.ebi.ac.uk/Tools/msa/clustalw2/).

To determine whether the prevalent p.R1939Q alleles are derived from a common founder, we conducted haplotype analysis. We genotyped single nucleotide polymorphisms (SNPs) with a minor allele frequency of >0.3 in the Japanese population and a microsatellite marker (D2S2350) spanning the *OTOF* locus and nearby genes on an ABI Genetic Analyzer 310 and Genescan 3.7 software (Applied Biosystems). Forty-four SNPs and the D2S2350 microsatellite marker in the vicinity of the mutation were genotyped in 11 AN patients who had p.R1939Q and in a part of their parents.

In six patients who did not have any mutations in *OTOF* and *GJB2* and three patients who were heterozygous for *OTOF* mutation without any mutations in *GJB2*, all coding exons and splice sites of *PJVK* were sequenced. Primer sequences were designed based on the reference sequence of *PJVK* (GenBank accession number NG_012186) and are listed in Table S2. Novelty of mutations and non-pathogenic variants found in the present study were examined in EVS (http://evs.gs.washington.edu/EVS/) and dbSNP

(http://www.ncbi.nlm.nih.gov/snp). The effect of an amino acid substitution was predicted using PolyPhen-2 software (http://genetics.bwh.harvard.edu/pph2/) and NNSPLICE 0.9 version (Berkley Drosophila Genome Project, http://www.fruitfly.org/seq_tools/splice.html) for the splice sites. The effect of p.D1842N was also analysed by modelling the three-dimensional structure of otoferlin using SWISS-MODEL (http://swissmodel.expasy.org/) (23).

Clinical examination and data analysis

Audiological tests included otoscopic examination and pure-tone audiometry with a diagnostic audiometer in a soundproof room following International Standards Organization standards. On the basis of pure-tone air-conduction thresholds, the degree of hearing loss was determined by the better ear pure-tone average across the frequencies 0.5, 1, 2, and 4 kHz, and it was classified as mild (20–40 dB), moderate (41–70 dB), severe (71–95 dB), or profound (>95 dB) according to the recommendations for the description of audiological data by the Hereditary Hearing Loss Homepage (http://hereditaryhearingloss.org).

Results

Genetic findings

Of 23 patients with a diagnosis of congenital or early-onset AN, 13 (56.5%) carried two pathogenic *OTOF* alleles, and 3 patients (13.0%) carried one pathogenic allele (Fig. 1: inner circle). In summary, ~70% of the patients had pathogenic *OTOF* alleles. Results of genotyping of the detected pathogenic *OTOF* alleles in 13 families carrying two pathogenic *OTOF* alleles (10 families in which two parents were examined and 3 families in which one parent was examined) were compatible with autosomal recessive inheritance in all these families. *OTOF* mutations consisted of three missense mutations, one frameshift mutation, two nonsense mutations, one non-stop mutation, and two putative splice site mutations (Tables 1 and 2). p.R1939Q was previously reported as a mutation and IVS47-2A>G was previously reported in dbSNP. Other seven *OTOF* mutations were novel. p.R1939Q was found in 43.5% of all alleles. We also identified 16 non-pathogenic *OTOF* variants, of which only p.P1697P was novel (Table 1). This variant did not change the score of splice site prediction. The location of each mutation in *OTOF* and the evolutionary conservation of the amino acids or nucleotides affected by the missense and putative splice site mutations are shown in Fig. 2a,b. The frequency of different *OTOF* genotypes is summarized in Fig. 1 (middle circle); 56.5% of the patients had p.R1939Q. In contrast, mutations other than p.R1939Q were confined to individual families. Previously, p.R1939Q was reported in one family with AN in the United States (19), and a different mutation in the same codon (p.R1939W) was reported in another family (16). Screening for the mutation

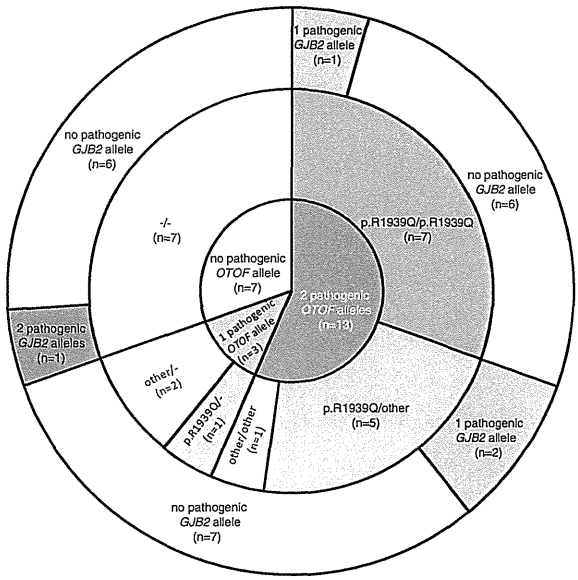

Fig. 1. Genetic backgrounds and frequency of different *OTOF* alleles in patients with congenital or early-onset auditory neuropathy (AN). (a) Distribution of patients carrying different pathogenic *OTOF* alleles (inner circle), *OTOF* genotypes (middle circle), and *GJB2* genotypes (outer circle). p.R1939Q indicates *OTOF* allele with p.R1939Q mutation; other indicates pathogenic *OTOF* alleles except for p.R1939Q allele; *n* indicates number of patients.

in 189 control subjects with normal hearing revealed only one heterozygous carrier. This mutation was predicted to be probably damaging variant according to PolyPhen-2.

The novel missense mutation p.D1842N was identified in a heterozygote without accompanying pathogenic alleles (patient 15). The mutation was predicted to be probably damaging variant according to PolyPhen-2. D1842 is located within the C2F domain, which is one of six calcium-binding modules (C2 domains) in otoferlin that are indispensable for otoferlin function. The predicted three-dimensional protein structure suggested that this mutation generates a repulsive force on calcium ions, resulting in reduced otoferlin activity (Fig. 3a–c). Another novel missense mutation, p.G541S, was identified as homozygous in a patient with parental consanguinity (patient 13). This mutation was predicted to be probably damaging variant according to PolyPhen-2 and involves a change from a non-polar residue to a polar residue in the C2C domain.

The c.1946-1965 del20 frameshift mutation truncates otoferlin at S648, causing a change in stop codon that adds six residues to the C terminus. Two nonsense mutations, p.Y474X and p.Y1822X, also truncate otoferlin. It is possible that these mutations trigger the nonsense-mediated decay response, by which aberrant mRNA is eliminated before translation (24). Even if the truncated proteins were produced, they would not function well because the mutations in c.1946-1965 del20, p.Y474X, and p.Y1822X disrupt three

Table 1. Mutations and non-pathogenic variants in congenital or early-onset auditory neuropathy

Types of variants	Location	Nucleotide variation	Predicted amino acid change	Allele frequency in normal controls	Novel or known
Mutations					
Missense substitution	Exon 15	c.1621G>A	p.G541S	0/376	Novel
	Exon 46	c.5524G>A	p.D1842N	0/376	Novel
	Exon 50	c.5816G>A	p.R1939Q	1/378	Known
Frameshift	Exon 17	c.1946-1965del20	p.R649PfsX5	0/192	Novel
Nonsense	Exon 14	c.1422T>A	p.Y474X	0/192	Novel
	Exon 46	c.5466C>G	p.Y1822X	0/192	Novel
Non-stop substitution	Exon 50	c.5992T>C	p.X1988RextX30	0/192	Novel
Putative splice site mutations					
	Exon 9 IVS	IVS9+5G>A		0/362	Novel
	Exon 47 IVS	IVS47-2A>G		0/190	Known
Non-pathogenic variants					
	Exon 2	c.129C>T	p.D43D	NT	Known
	Exon 3	c.145C>T	p.R49W	3/192	Known
	Exon 3	c.158C>T	p.A53V	75/192	Known
	Exon 4	c.244C>T	p.R82C	29/192	Known
	Exon 5	c.372A>G	p.T124T	NT	Known
	Exon 19	c.62C>T	p.P21L	172/172	Known
	Exon 23	c.2452C>T	p.R818W	0/188	Known
	Exon 24	c.2580C>G	p.V860V	NT	Known
	Exon 24	c.2613C>T	p.L861L	NT	Known
	Exon 25	c.2703G>A	p.S901S	NT	Known
	Exon 25	c.2736G>C	p.L912L	NT	Known
	Exon 41	c.4677G>A	p.V1559V	NT	Known
	Exon 41	c.4767C>T	p.R1589R	NT	Known
	Exon 43	c.5026C>T	p.R1676C	8/188	Known
	Exon 43	c.5091G>A	p.P1697P	NT	Novel
	Exon 45	c.5331C>T	p.D1777D	NT	Known

C2 domains, four C2 domains, and one C2 domain, respectively.

p.X1988RextX30, in which the stop codon is affected and 30 residues are added to the C terminus, accompanied p.R1939Q in a compound heterozygote (patient 12). Because the stop codon is separated by only one residue from the transmembrane domain, the additional C-terminal tail residues would interfere with anchoring to the membrane, which is critical for proper function. The three subjects with only one pathogenic *OTOF* allele (patient 14, patient 15, and patient 16) are likely to have mutations which could not be identified in the present study rather than just be coincidental carriers. Mutations which were not excluded in the present study include those in introns, a previously unknown exon, or a distant enhancer/promotor region as well as large deletions or other sequence rearrangements.

Screening of other genes revealed that one patient who did not have any mutations in *OTOF* was a compound heterozygote of *GJB2* mutations (patient 21). The AN phenotype has been reported in subjects with *GJB2* mutations (25). We identified three other patients with biallelic *OTOF* mutations that had heterozygous *GJB2* mutations, but they were considered to be coincidental. Distribution of patients carrying different pathogenic GJB2 alleles was shown in Fig. 1 (outer circle). None of the patients had A1555G or A3243G mitochondrial DNA mutations. Mutations in *PJVK* were not detected in six patients who did not have any mutations in *OTOF* or *GJB2* as well as in three patients who were heterozygous for *OTOF* mutation without mutations in *GJB2*.

All but one patient had a single haplotype associated with the p.R1939Q variant, which was not represented in 22 wild-type alleles in the parents, and representative SNPs and their allele frequencies as well as haplotypes are shown in Fig. 4a,b. Patient 2 had recombination of the same p.R1939Q-associated haplotype with the wild-type haplotype from his father. These results indicated that all the chromosomes carrying p.R1939Q were derived from a common ancestor.

Clinical findings

Clinical features of the patients are shown in Table 2. A consistent phenotype was present in seven patients carrying homozygous p.R1939Q and four patients who had heterozygous p.R1939Q accompanied by heterozygous truncating or putative splice site mutations. Patient 12, a compound heterozygote of p.R1939Q and a non-truncating mutation, showed a distinct phenoytpe. Patient 13, a homozygote of another non-truncating mutation, presented with temperature-sensitive AN.

Table 2. Genetic and clinical features of patients with congenital or early-onset auditory neuropathy

OTOF genotype[a]	Patient ID	Age, sex	*GJB2* genotype[a]	Degree of hearing loss (age of test)	Phenotype
p.R193Q/p.R1939Q					
	1	3, M	–/–	Profound (1 year 7 months)	NP, flat
	2	2, M	–/–	Profound (2 years 7 months)	NP, flat
	3	3, M	–/–	Profound (3 years 2 months)	NP, flat
	4	4, M	c.235delC/–	Profound (3 years 2 months)	NP, gently sloping
	5	2, F	–/–	profound (2 years 6 months)	NP, gently sloping
	6	2, M	–/–	Severe (2 years 10 months)	NP, flat
	7	2, M	–/–	Severe (1 year 9 months)	NP, flat
p.R1939Q/truncating or putative splice site[b]					
p.R1939Q/c.1946-1965del20	8	9, M	–/–	Unstable (2 years 10 months)	unstable, gently sloping
p.R1939Q/p.Y474X	9	2, M	–/–	Profound (1 year 7 months)	NP, flat
p.R1939Q/p.Y1822X	10	1, F	p.G45E+p.Y136X/–	Profound (2 years 0 month)	NP, flat
p.R1939Q/IVS9+5G>A	11	7, F	–/–	Profound (7 years 6 months)	NP, flat
p.R1939Q/non-truncating[c]					
p.R1939Q/p.X1988RextX30	12	29, F	p.V371/–	Moderate (29 years 1 month)	P, R: steeply sloping L: gently sloping
Non-truncating/non-truncating					
p.G541S/p.G541S	13	26, M	–/–	Mild[d] (25 years 11 months)	NP, flat
Various heterozygotes[e]					
p.R1939Q/–	14	5, F	–/–	Profound (5 years 10 months)	NP, flat
p.D1842N/–	15	2, F	–/–	Moderate (2 years 9 months)	NP, flat
IVS47-2A>G/–	16	6, F	–/–	Profound (5 years 11 months)	NP, flat
No mutations					
	17	4, F	–/–	Severe (4 years 8 months)	NP, gently sloping
	18	7, M	–/–	Profound (7 years 4 months)	NP, gently sloping
	19	6, F	–/–	Severe (5 years 7 months)	NP, R: gently sloping L: flat
	20	8, F	–/–	Profound (8 years 2 months)	NP, gently sloping
	21	3, F	p.235delC/c.176-191del16	Profound (3 years 1 month)	NP, flat
	22	7, F	–/–	Severe (7 years 10 months)	NP, flat
	23	2, M	–/–	Severe (1 year 8 months)	NP, flat

F, female; ID, identification number; M, male; NP, non-progressive; P, progressive; Phenotype (course of hearing loss and audiogram shape).
[a]No mutations.
[b]Truncating or putative splice site mutations.
[c]Non-truncating mutations.
[d]Temperature-sensitive auditory neuropathy.
[e]Mutations in heterozygotes without accompanying pathogenic mutations.

Patient 13 complained of difficulty in understanding conversation, and his hearing deteriorated when he became febrile or was exposed to loud noise according to his self-report. He explained that the deterioration varied from mild to complete loss of communication. Pure-tone audiometry when he was afebrile revealed mild hearing loss with a flat configuration. Among three patients who had only one pathogenic allele of *OTOF*, patient 15 carrying p.D1842N presented with moderate hearing loss, whereas patient 14 carrying p.R1939Q and patient 16 carrying IVS47-2A>G presented with profound hearing loss.

Discussion

The present study demonstrated biallelic *OTOF* mutations in 56.5% (13 of 23) of subjects with congenital or early-onset AN in Japanese population, indicating the most frequent cause associated with this type of AN. So far, biallelic *OTOF* mutations were identified in 22.2% (2 of 9) and 55% (11 of 20) of subjects with AN in American and Spanish studies, respectively (11, 12). In Brazilian population, 27.3% (3 of 11) of subjects with AN had *OTOF* mutations in two alleles (13). Taiwanese and Chinese subjects demonstrated that 18.2% (4 of 22)

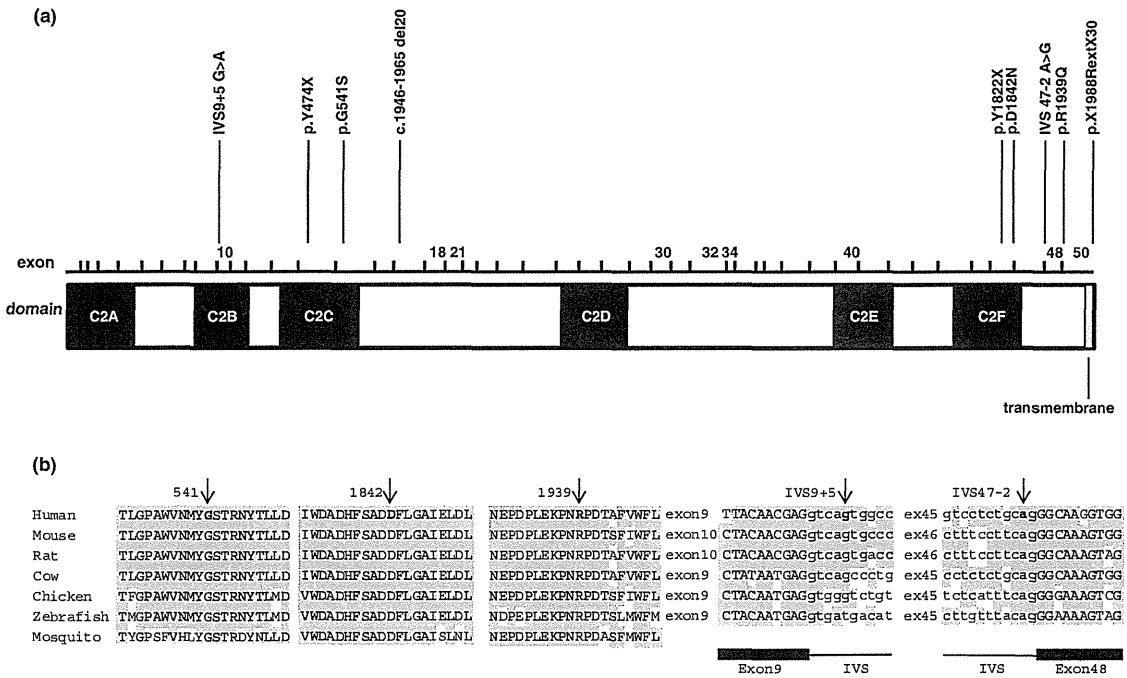

Fig. 2. The location of each mutation in *OTOF* and the evolutionary conservation of the amino acids or nucleotides affected by the missense and splice site mutations. (a) Location of mutations in the *OTOF* coding region of the cochlear isoform. Calcium-binding domains C2A through C2F are shown in black. (b) Multiple alignments of otoferlin orthologs at five non-contiguous regions and splice sites. Arrows indicate affected amino acids or nucleotides. Regions of amino acid and nucleotide sequence identity are shaded. Boundaries between introns and exons are indicated in the bottom. IVS indicates intervening sequence.

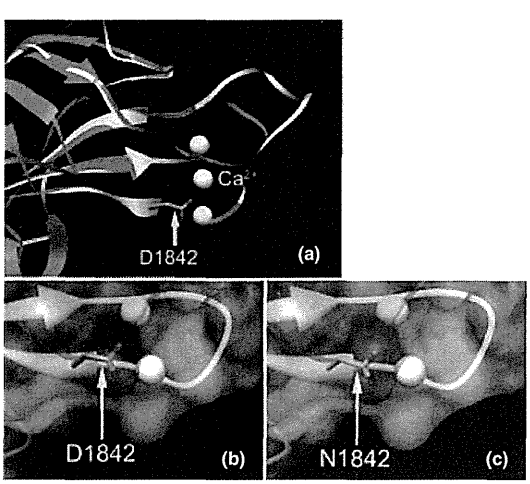

Fig. 3. Predicted three-dimensional protein structures of C2F domain in wild-type otoferlin and D1842N mutant otoferlin. (a) Ribbon model of the otoferlin C2F domain (white) superimposed onto that of the corresponding region of human protein kinase C gamma (hPKCγ, PDBID: 2UZP, chain A) which was selected as an optimal template (29.5% amino acid sequence identity) (magenta). Ca^{2+} is shown as a white sphere. The regions around D1842 of wild-type otoferlin (b) and N1842 of mutant otoferlin (c) are overlaid with their electrostatic surface potentials indicated by red (negative), blue (positive), and white (neutral). The side chains of both D1842 and N1842 are located very close (within 1.0 Å) to calcium ions. D1842N changes the electrostatic surface potential around the side chain from negative to positive in the cellular environment (pH = 7.4), and generate repulsive force on calcium ions.

and 1.4% (1 of 73), respectively, had biallelic *OTOF* mutations (14, 15).

The spectrum of *OTOF* mutations we identified differed significantly from those in other populations. Most reported *OTOF* mutations in the literature have been confined to individual families. An exception is p.Q829X, found in approximately 3% of autosomal recessive non-syndromic sensorineural hearing loss cases in the Spanish population (18). Recently, c.2905-2923delinsCTCCGAGCGCA and p.E1700Q were identified in four Argentinean families and four Taiwanese families, respectively (12, 14). In this study, p.R1939Q was detected in 13 families. Thus, p.R1939Q is now the second-most prevalent *OTOF* mutation reported. This mutation may be more common in Japan, as this mutation is found in only 1 of 10753 choromosomes in the European-American and African-American population by EVS. p.R1939Q was previously reported in one family in the United States, but the origin of the family was not detailed (19). Because no patients carrying p.R1939Q have been reported in Asian population except for the present study or in European population, this prevalent founder mutation appears to be an independent mutational event in Japanese.

Pathogenic *OTOF* mutations have been associated with stable, severe-to-profound sensorineural hearing loss with a few exceptions: c.2093+1G>T and p.P1987R were associated with stable, moderate-to-severe hearing loss (11, 19), p.E1700Q was associated with progressive, moderate-to-profound hearing

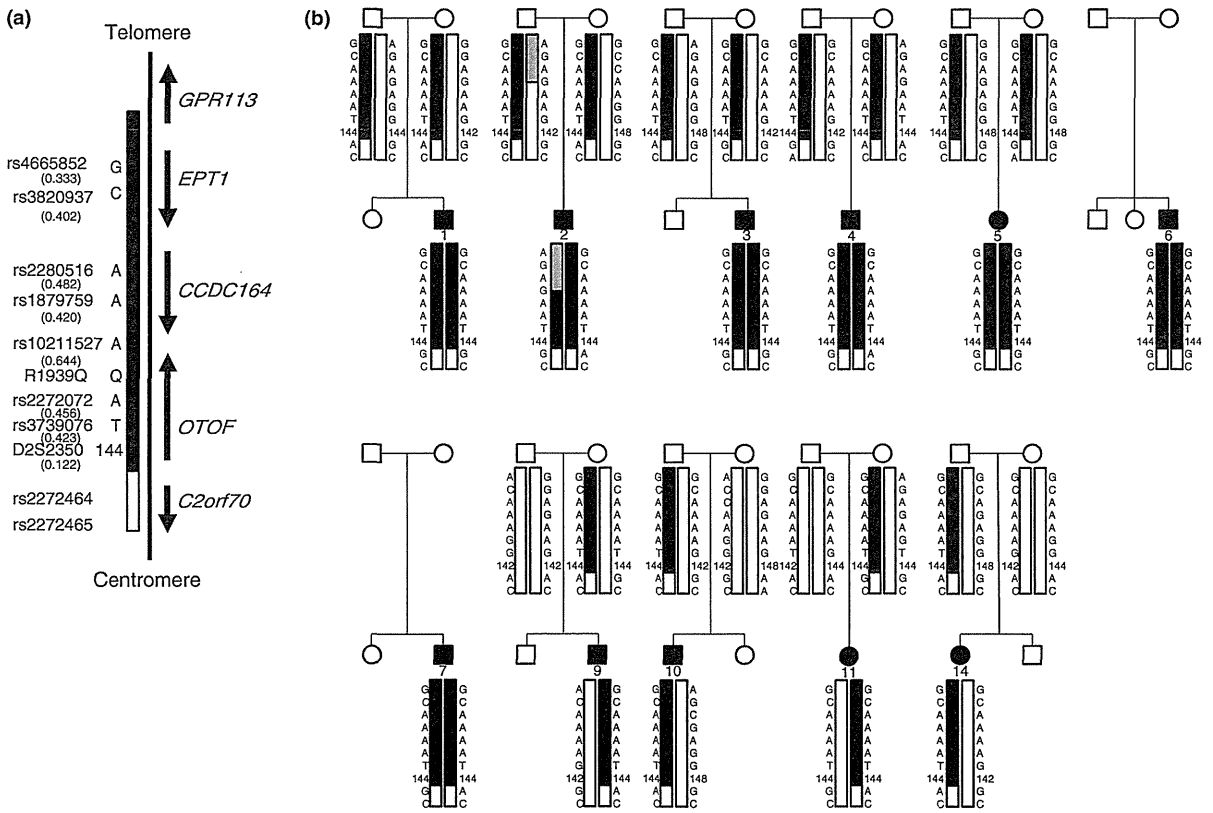

Fig. 4. Results of haplotype analysis of patients who had p.R1939Q alleles and their parents. (a) A part of tested single nucleotide polymorphisms (SNPs) and a microsatellite marker in relation to the genetic map around *OTOF* (chromosome 2p23.1). The region corresponding to the haplotype associated with the p.R1939Q mutation is indicated by black. Allele frequency of each SNP and a microsatellite marker is shown in a parenthesis. (b) Haplotypes of 11 auditory neuropathy (AN) patients with hearing loss who had p.R1939Q and their parents. The haplotype is indicated beside the vertical bars. The number under the symbol is the patient identification number in Table 2. A recombination point is indicated by grey in patient 2.

loss (14), and several mutations were associated with temperature-sensitive AN (11, 13, 15, 20). p.R1939Q homozygotes had a consistent phenotype of congenital or early-onset, stable, and severe-to-profound hearing loss with a flat or gently sloping audiogram. The same phenotype has also been reported in a family in United States, which included compound heterozygotes having p.R1939Q and a truncating mutation (19). Patients that were compound heterozygotes of p.R1939Q and truncating mutations or a putative splice site mutation also exhibited the similar phenotype in the present study. Thus, p.R1939Q variants are likely to cause severe impairment of otoferlin function. In contrast, a subject that was a compound heterozygote of p.R1939Q and a non-truncating mutation presented with a distinct phenotype of congenital or early-onset, progressive, moderate hearing loss with a steeply sloping or gently sloping audiogram. A homozygote of another non-truncating mutation also showed a distinct phenotype of temperature-sensitive AN. One of three patients who had only one allele of non-truncating mutation other than p.R1939Q presented with moderate hearing loss, whereas the other two subjects who had only one allele of p.R1939Q or a putative splice site mutation presented with profound hearing loss. These genotype–phenotype correlations of *OTOF* were similar to those of *GJB2*, i.e., more severe hearing loss was observed in subjects homozygous for truncating mutations than in subjects homozygous for non-truncating mutations, and more severe hearing loss was observed in subjects homozygous for a frameshift mutation (35delG) than in subjects compound heterozygous for the 35delG and other mutations (26, 27).

A patient with temperature-sensitive AN with a specific *OTOF* mutation was found in the present study. So far, temperature-sensitive AN has been observed in two siblings with heterozygous p.I515T without an accompanying pathogenic allele (11), three siblings with homozygous p.E1804del (20), a compound heterozygote with c.2975-2978delAG and p.R1607W (15), and a compound heterozygote with p.G614E and p.R1080P (13). The patient in this study had biallelic mutations affecting residues specific to the long isoform. Previously, two subjects showed biallelic mutations affecting this region, but they were not tested for OAE (16, 17). Thus, the present patient is the first case with biallelic mutations in this region, which indicates that mutations in the *OTOF* long isoform alone are able to cause AN.